

Technical Details for "Quantum impurities in channel mixing baths"

Jin-Guo Liu,¹ Da Wang,¹ and Qiang-Hua Wang^{1,2,*}

¹*National Laboratory of Solid State Microstructures & School of Physics, Nanjing University, Nanjing, 210093, China*

²*Collaborative Innovation Center of Advanced Microstructures, Nanjing University, Nanjing 210093, China*

(Dated: September 8, 2015)

I. DISCRETIZATION

A. Pin down the discretization mesh points

Before reading this manuscript, it is highly recommended to read Ref.¹⁻³ to get some basic understanding of "continuous index x " and mapping criterias. All discretization schemes starts from pinning down the discretization mesh points, which are essential for the validity of NRG iteration. A variety of schemes are available for the conventional superconducting problem,

1. *log scale*: $\varepsilon(x) = \min[(D - \Delta)\Lambda^{2-|x|} + \Delta, D] \text{sign}(x)$, here we introduced a gap Δ to avoid empty hybridization functions which will induce "big" problems during discretization.
2. *superconducting-optimized log scale*: $\varepsilon(x) = \sqrt{\min[D_0\Lambda^{2-|x|}, D_0]^2 + \Delta^2} \text{sign}(x)$, with $D = \sqrt{D_0^2 + \Delta^2}$, which is derived from the early discretization schemes for normal part^{4,5}.
3. *adaptive scale*: An adaptive discretization scheme that will put more ticks at energy scales with stronger hybridization strength³, the hybridization strength could be defined as $\mathcal{S}(\omega) = \sqrt{\sum_n \rho_n(\omega)^2}$, see Ref.³ for details of numerical implementation(you can find a software pack in this paper).

In the case of getting lowest energies of normal superconducting model, these discretization schemes seen to have little effect to the final result(600 states are kept). The most prominent effects lies in the temperature dependant observables.

B. Pin down the representative energies and hopping terms

In order to get the representative energy $E(x)$ and hopping $T(x)$ for each energy scale(interval) $I(x) \equiv \varepsilon(x) \sim \varepsilon(x + \text{sgn}(x))$, we perform eigenvalue decomposition to the hybridization matrix(thanks to the hermicity), here we take a 2×2 hybridization matrix as an example.

$$\mathcal{D}(\omega) = U(\omega) \begin{pmatrix} \rho_1 & 0 \\ 0 & \rho_2 \end{pmatrix} U(\omega)^\dagger \quad (1)$$

Representative energy $\epsilon_{1,2}(x)$ and hopping $t_{1,2}(x)$ for each channel can be decided by following the procedure in Ref.^{2,3}, In practice, we have much stable method to calculate the differential equations in Ref.^{2,3}. Considering the positive branch, we have the following relation of ϵ and x

$$\int_x^1 t_n^2(x') dx' = - \int_\epsilon^1 \rho(\epsilon') d\epsilon' \quad (2)$$

Let $R(\omega) = \int_0^\omega \rho(\omega) d\omega$

$$\begin{aligned} \int_1^x R(\varepsilon(x')) - R(\varepsilon(x' + 1)) dx' &= R(D) - R(\epsilon) \\ \int_1^2 R(\varepsilon(x')) dx' - \int_x^{x+1} R(\varepsilon(x')) dx' &= R(D) - R(\epsilon) \end{aligned} \quad (3)$$

Note that $x = D$ for $x \in [1, 2]$, we have

$$\int_x^{x+1} R(\varepsilon(x')) dx' = R(\epsilon) \quad (4)$$

this is why we say $\varepsilon(x+1) < \epsilon(x) < \varepsilon(x)$ in the main text.

Then we get

$$\begin{aligned}\mathcal{D}(\omega)_{ij} &= \sum_{n=1,2} U(\omega)_{in} \left(\int_1^\infty t_n(x)^2 \delta(\omega - \epsilon_n(x)) dx \right) U(\omega)_{nj}^\dagger \\ &= \sum_{n=1,2} \int_1^\infty \tilde{U}(x)_{in} t_n(x) \delta(\omega - \epsilon_n(x)) t_n(x) \tilde{U}(x)_{nj}^\dagger dx\end{aligned}\tag{5}$$

In the second line of Eq.5, we absorbed $U(\omega)$ into the inner part of integral which can be done by considering the feature of $\delta(\omega - \epsilon_n(x))$. Here, we have defined a new matrix $\tilde{U}(x)_{ij} = U(\epsilon_j(x))_{ij}$ which is not unitary in general.

In the matrix representation,

$$\begin{aligned}\mathcal{D}(\omega) &= \int_1^\infty T(x) \delta(\omega - E(x)) T(x)^\dagger dx \\ T^\dagger(x) &\equiv \tilde{U}(x) \begin{pmatrix} t_1(x) & \mathbf{0} \\ \mathbf{0} & t_2(x) \end{pmatrix} \\ E(x) &\equiv \begin{pmatrix} \epsilon_1(x) & \mathbf{0} \\ \mathbf{0} & \epsilon_2(x) \end{pmatrix}\end{aligned}\tag{6}$$

Above method also apply for the negative branch.

A question may arise that whether this replacement is numerically stable? In other words, will the overall phase of $U(\omega)$ affect the result? In fact, the 2×2 hybridization function could be decomposed analytically, the analytical behavior of $U(\omega)$ is guaranteed. Numerical decomposition is also tested, it should be noticed that in the special case of band degeneracy, the choice of $U(\omega)$ is random in the degenerate subspace. In this case, you should take columns of these degenerate bands within the same $U(\omega)$, degeneracy detection is required!

In practice, we perform interpolation over discrete datas of 4-pauli-components of $\mathcal{D}(\omega)$, Here, the number of ω should be taken $\geq 10^5$ for satisfactory results. With the above interpolation, $U(\omega)$ could be obtained directly from the 4-pauli-components at ω .

II. BLOCK-TRIDIAGONALIZATION

The obtaining of the first site have been discussed with enough details in the main text. U_0^\dagger is now the initial vector which is a $2JI \times I$ "unitary matrix" (orthogonal in columns but do not form a complete set). And the Hamiltonian - matrix for tridiagonalization

$$H_z = \begin{pmatrix} \mathbf{E}(1+z) & \mathbf{0} & \mathbf{0} & \mathbf{0} & \dots & \mathbf{0} \\ \mathbf{0} & \mathbf{E}(-1-z) & \mathbf{0} & \mathbf{0} & \dots & \mathbf{0} \\ \mathbf{0} & \mathbf{0} & \mathbf{E}(2+z) & \mathbf{0} & \dots & \mathbf{0} \\ \mathbf{0} & \mathbf{0} & \mathbf{0} & \mathbf{E}(-2-z) & \dots & \mathbf{0} \\ \vdots & \vdots & \vdots & \vdots & \ddots & \vdots \\ \mathbf{0} & \mathbf{0} & \mathbf{0} & \mathbf{0} & \dots & \mathbf{E}(-N-z) \end{pmatrix}\tag{7}$$

is $2JI \times 2JI$.

The algorithm for block-tridiagonalization with block size $I \times I$ and Hamiltonian dimension $2JI \times 2JI$,⁶

```

 $Q_0 = \mathbf{0}$ 
 $Q_1 = (2JI \times I \text{ initial vector with columns orthonormalized, here } U_0^\dagger.)$ 
 $B_1 = \mathbf{0}$ 
for  $j = 1, 2, \dots, J - 1$ 
     $U_j = H_z Q_j - Q_{j-1} B_j^\dagger$ 
     $A_j = Q_j^\dagger U_j$ 
     $R_{j+1} = U_j - Q_j A_j$ 
     $Q_{j+1} B_{j+1} = R_j$  (QR factorization of  $w_j$ , with  $Q_{j+1}$  orthogonal and  $B_{j+1}$  upper triangular.)
endfor
 $A_J = Q_J^\dagger H_z Q_J$ 
return

```

The matrices Q_j , U_j , R_j for $j = 1, 2, \dots, m - 1$ are $n \times p$, whereas A_j (on-site energy of chain) and B_j (hopping term of chain) are $p \times p$, with A_j Hermitian. Note that the above procedure is stopped after $J - 1$ steps as convention.

A. QR decomposition

We notice that all the QR decomposition should be done analytically for the purpose of arbitrary high precision requirement. Stable arbitrary high precision packages "MPFR/MPC" are available for C++ coder, and its python wrapper "gmpy2" is also available for Python coder. In our calculation, 6000 bits(1808 digits) precision is used, which is suitable in most cases.

The algorithm of QR decomposition for $n \times p$ ($n \geq p$) matrix A is:

```

for  $j = 1, 2, \dots, p$ 
     $U_i = A[:, j]$  (take  $j$ -th column of  $A$ )
     $U_i = U_i - Q Q^\dagger U_i$ 
     $U_i = U_i / |U_i|$ 
     $Q = (Q, U_i)$  (concatenate  $Q$  and  $U_i$  by column)
endfor
 $R = Q^\dagger A$ 
return Q, R

```

III. CHECK FOR MAPPING

We discretize the s-wave superconducting bath as discussed in the main text. We set $\pi\Gamma = 0.5$ and $\Delta = 0.1$, and take $D = \sqrt{1 + \Delta^2}$ as the cutoff energy due to the pairing gap. To check the precision of this mapping, we use the resulting discretized model to recalculate $\mathcal{D}(\omega) = d_0(\omega)\sigma_0 + d_x\sigma_x(\omega)$, and we compare them to the analytical results in Fig.1(a). We see excellent agreement in the low energy window. The deviation at the band edges is an artifact due to the larger smearing factor we used for larger energies.

We proceed to perform the mapping to the Wilson chain, and we use this chain to calculate $d_{0,x}(\omega)$ again numerically by means of recursive Green's function⁷, and compare to the analytical results in Fig.1(b). The agreement within each panel and the consistency between the two panels reveal the nice accuracy and consistency of our two-stage mapping schemes.

IV. SOURCE CODE

We have uploaded our program(mapping part) and technical details to the internet. https://github.com/GiggleLiu/nrg_mapping

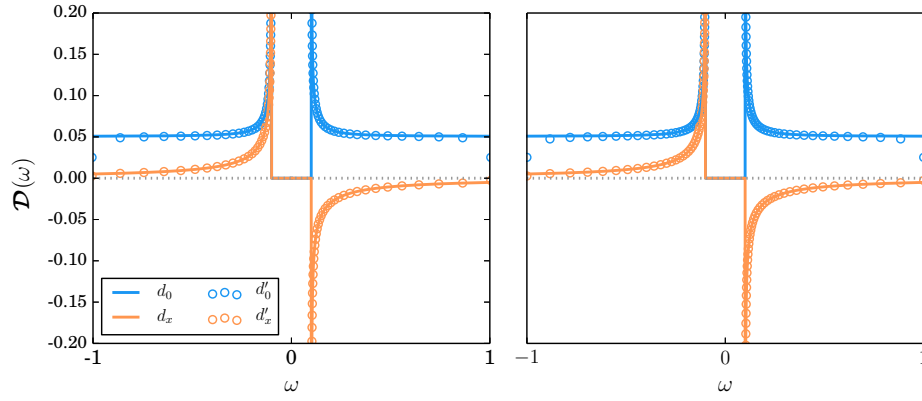


FIG. 1. Comparison of the analytical $d_0(\omega)$ and $d_x(\omega)$ (solid lines) and numerical results $d'_0(\omega)$ and $d'_x(\omega)$ (symbols) obtained from (a) the discrete bath and (b) the open Wilson chain. The scaling parameter $\Lambda = 3$ and the number of block-Lanczos iterations is $J = 25$. The result is averaged over 50 twisting factors η uniformly distributed in $(0, 1]$.

This program requires python environment and supports only 2 x 2 hybridization function. However, it can be easily extended to any dimension as long as you are familiar with python.

Also, you will find an interesting test and an API document in this repo.

* dg1422033@smail.nju.edu.cn

¹ V. L. Campo and L. N. Oliveira, *Phys. Rev. B* **72**, 104432 (2005).

² R. Žitko and T. Pruschke, *Phys. Rev. B* **79**, 085106 (2009).

³ R. Žitko, *Comp. Phys. Comm.* **180**, 1271 (2009).

⁴ K. Satori, H. Shiba, O. Sakai, and Y. Shimizu, *J. Phys. Soc. Jpn* **61**, 3239 (1992); O. Sakai, Y. Shimizu, H. Shiba, and K. Satori, *J. Phys. Soc. Jpn* **62**, 3181 (1993).

⁵ T. Yoshioka and Y. Ohashi, *J. Phys. Soc. Jpn* **69**, 1812 (2000).

⁶ R. G. Grimes, J. G. Lewis, and H. D. Simon, *SIAM J. Matrix Anal. Appl.* **15**, 228 (1994).